ADVANCED OPTICAL MATERIALS

www.advopticalmat.de

Controllable Photoluminescence Behaviors of Amphiphilic Porphyrin Supramolecular Assembly Mediated by Cyclodextrins

*Guoxing Liu, Ying-Ming Zhang, Xiufang Xu, Lu Zhang, Qilin Yu, Qian Zhao, Chaoyue Zhao, and Yu Liu**

Tunable photoluminescence nanomaterials have aroused increasing interest from researchers recently due to their application in bioimaging, photodynamic therapy, and energy conversion. Herein, an artificial ternary nanosystem comprised of dithienylethene-bridged bis(permethyl-β-CD)s, dodecyl-bearing porphyrin, and amphipathic near-infrared (NIR) cyanine fluorochrome is conveniently constructed by rationally designing the host/guest components, dimensions, and properties. In this system, an effective energy transfer (ET) from porphyrin to cyanine fluorochrome leads to the dramatic enhancement of NIR fluorescence intensity and more crucially, this process can be efficiently regulated by distinct light input, achieving photoswitching ET-NIR fluorescence in aqueous media.

Stimuli-responsive nanosystems formed by multicomponent supramolecular self-organization are of great interest, due to their simple composition, easy adjustability, and good reproducibility. As one of the most important photophysical tools in stimuli-responsive photoluminescent materials, energy transfer (ET) has been widely applied in biological sensing,[1] photodynamic therapy,[2] photocontrolling the generation of singlet oxygen,[3] upconversion luminescent devices,[4] and light-tunable fluorescent supramolecular systems.[5] Among various fluorophores to achieve ET process applied in biological sensing, near-infrared (NIR) fluorochromes are preferred for imaging living cells and tissues, because they offer low phototoxicity to cells, minimal interference by the hemoglobin absorption, low autofluorescence, and good tissue penetration.[6] Furthermore, light is considered as a more attractive candidate for its noninvasiveness, easy controllability, low cost, and ubiquity, compared with other various external stimuli.[7] Therefore, the combination of light input and NIR labels is expected to provide a new quick access to the fabrication of advanced optically functional materials. However, constructing photoadjustable NIR photoluminescent nanosystem that incorporates multiple NIR fluorochromes and works in aqueous media is not an easy task and, indeed, has never been achieved, to the best of our knowledge.

In the present work, we employed supramolecular methodology to construct a photoresponsive nanoassembly that emits photochemically switchable NIR fluorescence in water. Our rationally designed ternary nanosystem, incorporating dithienylethene, porphyrin, and cyanine dye as the essential components, has several inherent advantages: (1) Dithienylethenes can undergo reversible cyclization/cycloreversion upon distinct light irradiation and constitute a key component in photoswitchable molecular devices,[8] (2) Porphyrins, often used as photosensitizers in biomedical field, can be supramolecularly functionalized by the noncovalent association with permethyl-β-cyclodextrins (PMCD);[9] (3) Cyanine dye-5 (Cy) is an excellent NIR fluorochrome frequently used in cellular imaging because of its chemical stability and high fluorescence quantum yield.[10] Thus, the rational conjugation of these components is expected to bring about a breakthrough in photoswitchable biomaterials. In our approach to realize such an intelligent system, the above-mentioned modules were incorporated in a sophisticated manner to create an unprecedented light-responsive supramolecular assembly that exhibits reversible photoswitching fluorescence resonance energy transfer (FRET) behaviors in the NIR region (**Scheme 1**).

Dithienylethene-bridged bis(permethyl-β-CD)s (**1**) (Scheme S1 and Figures S1–S4, Supporting Information) exhibited excellent photochromism reversibility in water. As shown in **Figure 1**a, the open-form of the molecular switch (OF-**1**) gave an absorption maximum at 292 nm ($\varepsilon = 4.36 \times 10^4$ L mol^{-1} cm^{-1}), while a new absorption peak appeared at 592 nm ($\varepsilon = 1.58 \times 10^4$ M^{-1} cm^{-1}) with an isosbestic point at 319 nm upon UV irradiation at 254 nm with accompanying color change from colorless to blue (Figure 1a, inset), as a consequence of the photocyclization of the dithienylethene moiety to the closed-form (CF-**1**). The

Dr. G. Liu, Dr. Y.-M. Zhang, Prof. X. Xu, L. Zhang, Dr. Q. Yu, Q. Zhao, C. Zhao, Prof. Y. Liu
College of Chemistry
State Key Laboratory of Elemento-Organic Chemistry
Nankai University
Tianjin 300071, P. R. China
E-mail: yuliu@nankai.edu.cn
Prof. Y. Liu
Collaborative Innovation Center of Chemical Science and Engineering
Nankai University
Tianjin 300071, P. R. China
The ORCID identification number(s) for the author(s) of this article can be found under https://doi.org/10.1002/adom.201700770.

DOI: 10.1002/adom.201700770

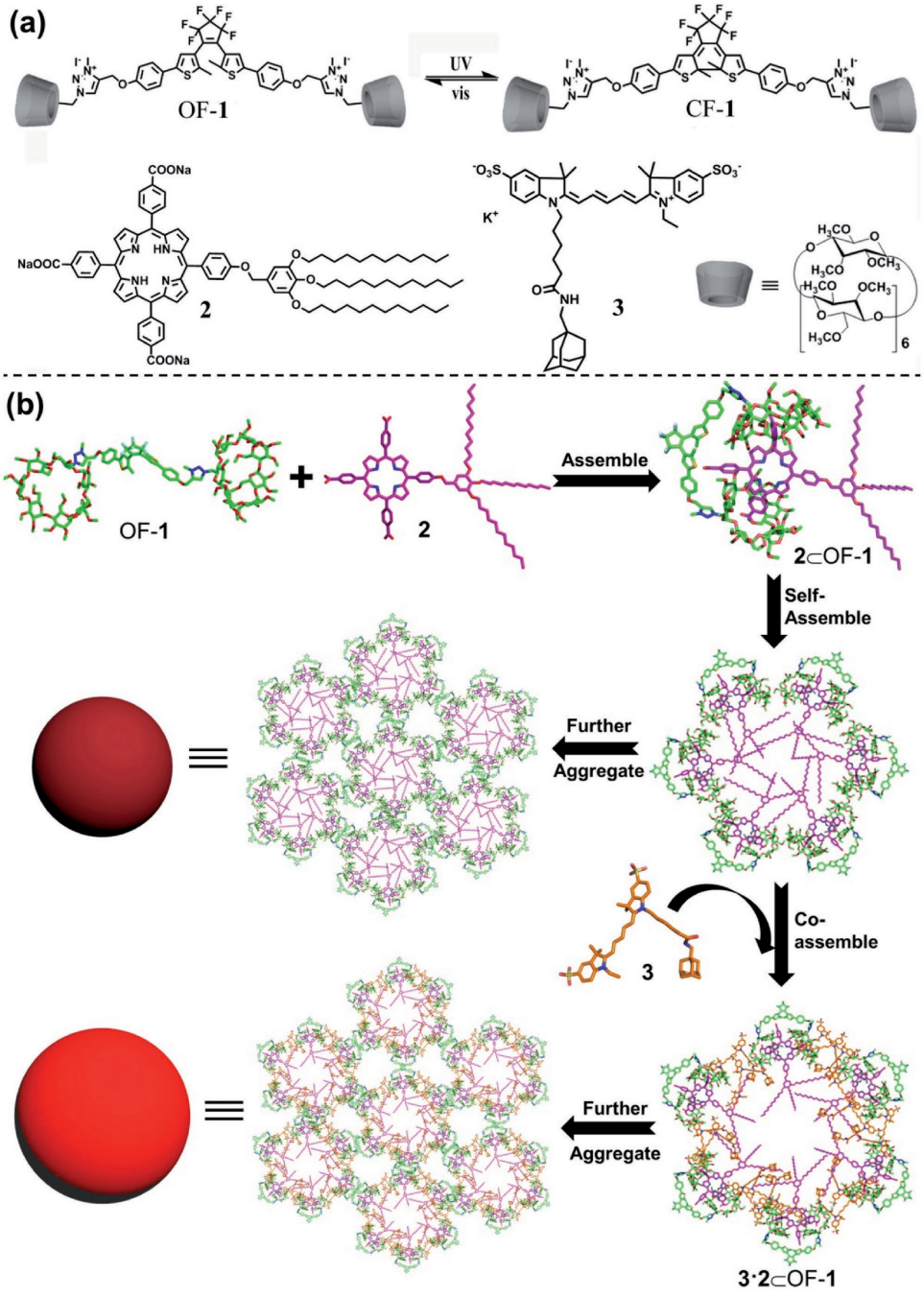

Scheme 1. a) Chemical structures of the dithienylethene-bridged PMCDs (**1**), amphiphilic porphyrin (**2**) and cyanine dye (**3**). b) Schematic illustration of spherical nanoparticles formed by **2**⊂OF-**1** and **3**·**2**⊂OF-**1** assemblies.

conversion was determined to be 92% by NMR spectral examination of the irradiated sample (Figure S5, Supporting Information). Photoirradiation at >450 nm of this sample containing CF-**1** led to a complete recovery of the original UV–vis and NMR spectra OF-**1** (Figures 1a and S6, Supporting Information), indicating reversible photocyclization/reversion between the open- and the closed-form as illustrated in Scheme 1a. Crucially, this photochromic switch showed a good reproducibility and no apparent deterioration could be observed even after repeating the cycles for at least ten times (Figure S7, Supporting Information). The photocyclization quantum yield (Φ_{o-c}) and the photo-cycloreversion quantum yield (Φ_{c-o}) of host **1** were determined to be 0.59 and 0.0056, respectively (Table S1, Supporting Information).

The introduction of PMCD units and triazolium cations is expected to endow host **1** with a good water-solubility and allow the two PMCDs to hold water-soluble porphyrins with extraordinary affinities.[11] Indeed, these inventions enabled the

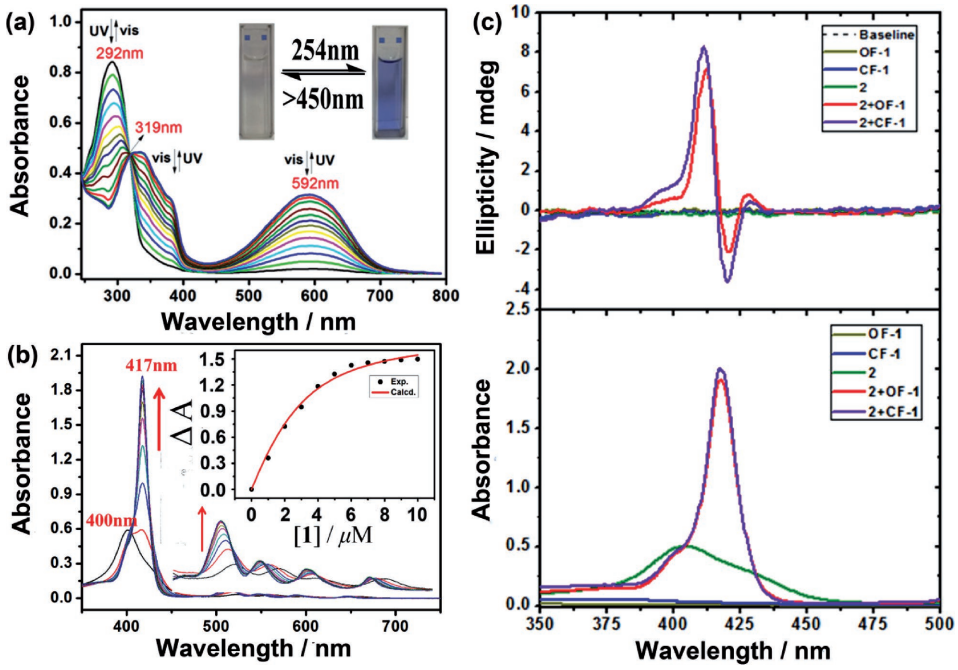

Figure 1. a) UV–vis spectral changes of **1** (20×10^{-6} M) in water upon irradiation at 254 nm and at >450 nm. b) UV–vis titration spectra of **2** (5×10^{-6} M) upon addition of OF-**1** ((0–10) $\times 10^{-6}$ M) in PBS (pH 7.2). Inset: Nonlinear least-squares fit of the absorbance changes (ΔA) at 417 nm to determine the complex stability constant (K_S) as 7.5×10^5 M^{-1}. c) Circular dichroism and UV–vis spectra of OF-**1**, CF-**1**, **2**, **2**⊂OF-**1**, and **2**⊂CF-**1** in PBS (pH 7.2); [**1**] = [**2**] = 5×10^{-6} M; path length: 10 mm.

facile construction of supramolecular assembly **2**⊂**1** by simply mixing host **1** and water-soluble porphyrin **2** in aqueous solution. Thus, a Job plot for the complexation of **2** with **1** revealed the 1:1 host–guest stoichiometry, exhibiting a peak at molar fraction 0.5 (Figure S8, Supporting Information) and the complex stability constant (K_S) was determined to be 7.5×10^5 M^{-1} by UV–vis spectral titration, where the absorbance changes upon stepwise addition of OF-**1** to an aqueous phosphate buffer solution (PBS, pH = 7.2) of **2** were analyzed by using the nonlinear least-squares fitting method[12] (Figure 1b). The K_S value thus obtained is comparable to those reported in the previous papers.[9,11] Moreover, in circular dichroism (CD) spectral examinations in PBS, although **2**, OF-**1**, and CF-**1** were CD-silent, equally strong bisignate Cotton effect signals were induced in the Soret band of **2** upon addition of OF-**1** and CF-**1** (Figure 1c, top), verifying the formation of **2**⊂OF-**1** and **2**⊂CF-**1** complexes.

Significantly, the fluorescence intensity of **2** was greatly enhanced by a factor of up to 120 upon addition of nonluminous OF-**1** (Figures 2a). Visually, the addition of OF-**1** turned on the red fluorescence of **2** upon formation of assembly **2**⊂OF-**1**, enabling naked-eye observation (**Figure 2**a, inset). More quantitatively, the fluorescence quantum yield (Φ_F) was greatly enhanced from <0.001 to 0.063 and the fluorescence lifetime (τ) of **2** was elongated from 0.8 to 11.8 ns upon formation of **2**⊂OF-**1** (see Figure S9a, Table S2, and the relevant discussion in the Supporting Information). In the absence of host **1**, the fluorescence of porphyrin **2** is suppressed due to H-aggregates by intermolecular π–π and hydrophobic interaction.[13] However, upon inclusion by the PMCD cavities of OF-**1**, the H-aggregates loosen or partially dissociate and the strong fluorescence of **2** revives.

The structural information was obtained for **2**⊂OF-**1** assembly by transmission electron microscopy (TEM) and dynamic light scattering (DLS) experiments. As discerned from the TEM image (Figure S10a, Supporting Information), many quasi-spherical nanostructures were observed with an average diameter of 100 nm, which is appreciably smaller than the hydrodynamic diameter (D_h = 158 nm) determined by DLS because of the shrinking of nanoparticles upon air-drying in the sample preparation for TEM (Figure S10b, Supporting Information).[14] Based on these spectroscopic, optimized structural (Figure S12, Supporting Information), and morphological analyses, a plausible illustration of spherical nanoparticles **2**⊂OF-**1** is given in Scheme 1b, which is consistent with the previous results.[9b]

It is well known that FRET process via the Förster mechanism is facilitated by a good spectral overlap of the donor emission with the acceptor absorption.[15] As can be seen from Figure S11a in the Supporting Information, **2**⊂OF-**1** assembly fluoresces at 647 and 714 nm, but OF-**1** does not absorb light in this region and hence no FRET process is expected to occur from **2** to OF-**1**. However, when **2**⊂OF-**1** assembly was irradiated at 254 nm for 28 s, the fluorescence of the assembly was strongly quenched by 96% (Figure 2b). Simultaneously, the Φ_F was reduced to <0.001 (Table S2, Supporting Information) and the red fluorescence became almost invisible to the naked eyes. The τ of **2**⊂OF-**1** was also significantly shortened from 11.8 to 0.8 ns upon UV irradiation (Figure S9b; Table S2, Supporting Information). These observations jointly indicate the occurrence of the FRET from **2** (donor) to CF-**1** (acceptor) due to the good spectral overlap of the fluorescence of **2** with the absorption of CF-**1** (Figure S11a, Supporting Information) and the

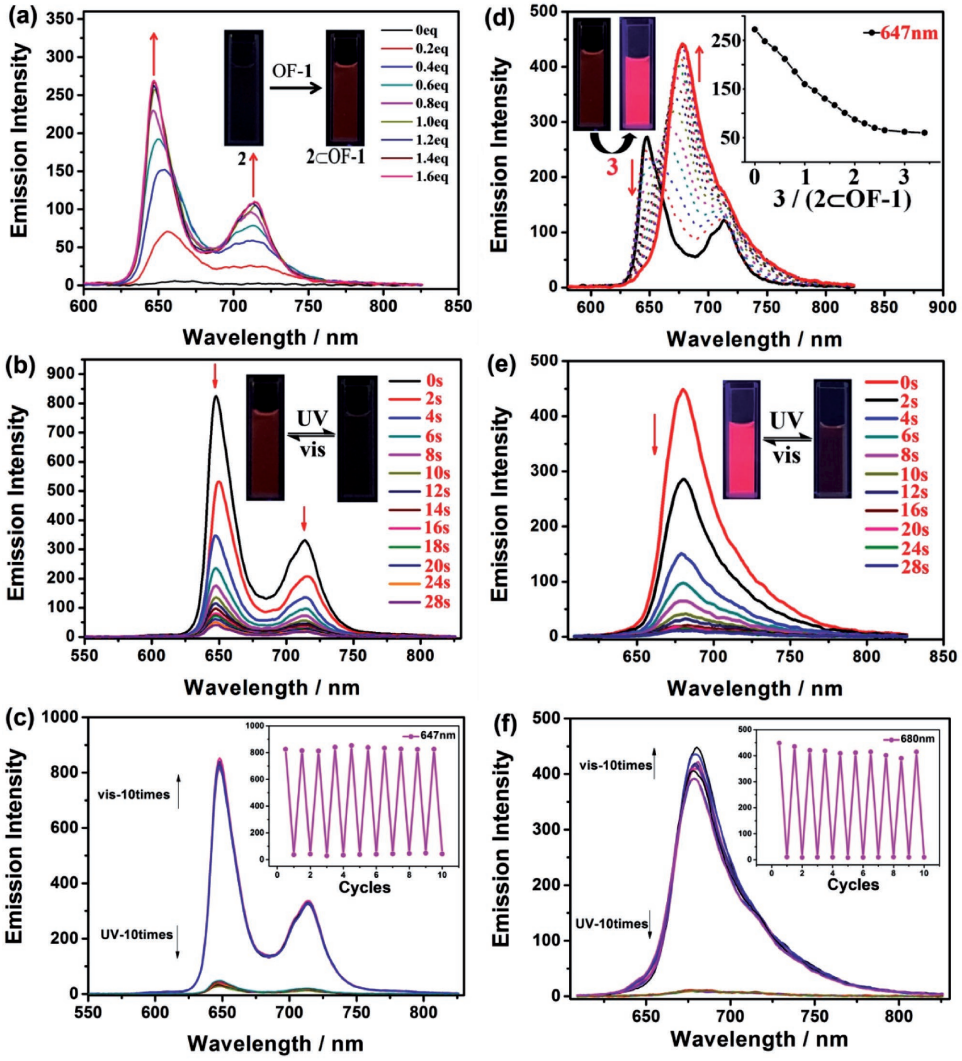

Figure 2. a) Fluorescence spectral variation of **2** (2.5×10^{-6} M) upon addition of OF-**1** ((0–4) $\times 10^{-6}$ M) in PBS (pH 7.2); slit = 5, 5. b) Fluorescence spectral variation of assembly **2**⊂OF-**1** upon irradiation with 254 nm light; slit = 5, 5. c) Fluorescence spectra and (inset) intensity changes at 647 nm for **2**⊂OF-**1** observed upon alternating UV (254 nm) and visible-light (>450 nm) irradiation. [**1**] = [**2**] = 5×10^{-6} M; slit = 10, 5. d) Fluorescence spectral variation of **2**⊂OF-**1** ([**1**] = [**2**] = 5×10^{-6} M) upon addition of **3** ((0–17) $\times 10^{-6}$ M); slit = 5, 5. e) Fluorescence spectral variation of assembly **3**·**2**⊂OF-**1** upon irradiation at 254 nm. [**3**] = [**2**] × 3 = [**1**] × 3 = 15×10^{-6} M; slit = 5, 5. f) Fluorescence spectra and (inset) intensity changes at 680 nm for **2**⊂OF-**1** observed upon alternating UV (254 nm) and visible light (>450 nm) irradiation; [**3**] = [**2**] × 3 = [**1**] × 3 = 15×10^{-6} M; slit = 5, 5 (excitation at 417 nm).

close donor–acceptor distance in **2**⊂CF-**1** complex. The center-to-center distance (r_{DA}) between CF-**1** and porphyrin core of **2** was estimated as 1.38 nm by using the semiempirical AM1 method implemented in Gaussian 09, which is well within the range of the Förster radius (R_0 < 10 nm) to facilitate the energy transfer channel (Figure S12d, Supporting Information).[16] The light-controlled FRET efficiency of the **2**⊂**1** assembly was determined as 96% from the fluorescence intensity change at 647 nm (Table S3, Supporting Information), which was well consistent with the one calculated by the excitation spectra of **2**⊂OF-**1** and **2**⊂CF-**1** (Figures S11 and S20, Supporting Information).

Furthermore, the quenched fluorescence of porphyrin in **2**⊂**1** complex was completely recovered to its original level upon continuous irradiation by the visible light (>450 nm) for 440 s (Figure S13, Supporting Information), indicating inhibition of the FRET process from **2** to **1**. This result is attributable to the reverse photoisomerization from CF-**1** to OF-**1** that has an excitation energy mismatched with the emission energy of **2**⊂PMCD complex. Other spectroscopic examinations and lifetime measurements also supported the emission recovery (Figure 2b; Table S2, Supporting Information). Significantly, this light-driven fluorescence switching cycle was repeatable for at least ten times without any fatigue (Figures 2c). Overall, the **2**⊂**1** nanoarchitecture is endowed with the light-controllable fluorescence switching ability in water, to which the reversible photoisomerization between OF-**1** and CF-**1**, the tunable spectral overlap of the emission of **2**⊂PMCD with the absorption of **1** and the appropriate donor–acceptor distance between **1** and **2** jointly contribute (**Scheme 2**, left). However, the fluorescent

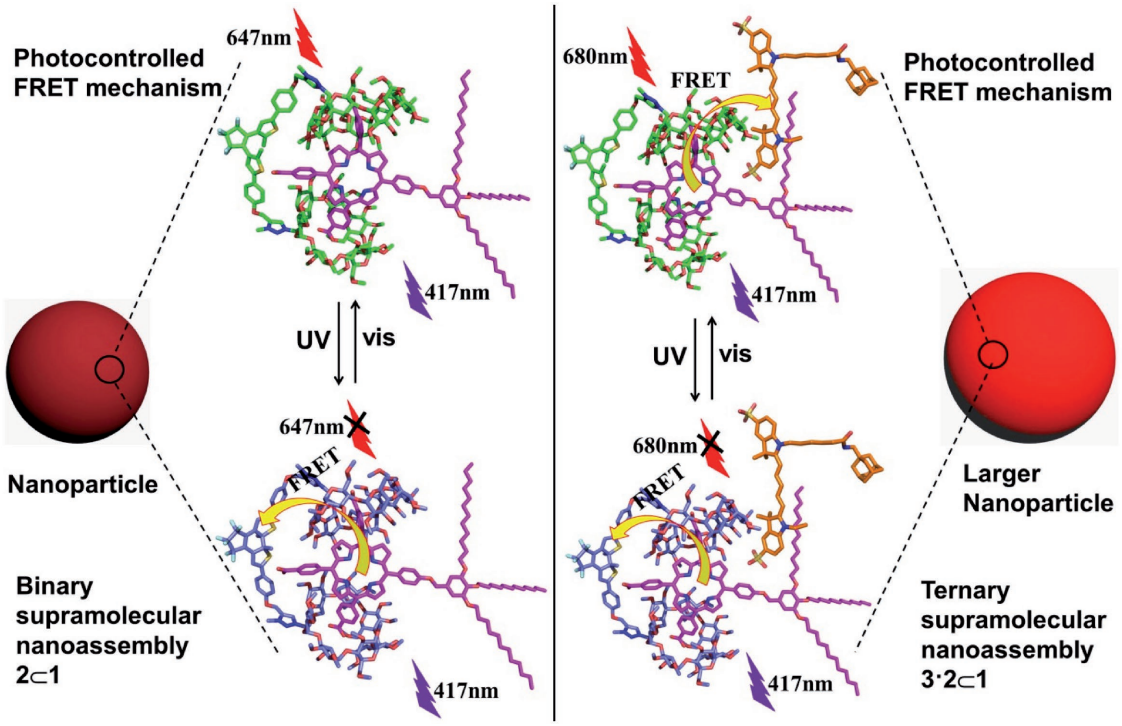

Scheme 2. Schematic illustration of the photocontrolled energy transfer process in binary assembly **2⊂1** (left) and ternary assembly **3·2⊂1** (right).

intensity and quantum yield of assembly **2⊂OF-1** are inferior, resulting in the limitation of its further application in photoluminescent materials.

Benefiting from our elaborate design, the structural feature of **2⊂1** assembly, possessing hydrophobic environment because of the long alkyl chains and the π-conjugated skeleton in amphipathic porphyrin **2**, could incorporate some water-repelling or amphiphilic fluorochromes with high quantum yield in its hydrophobic region.[17] We chose an adamantane-modified cyanine dye-5 (Cy-AD **3**, as shown in Scheme 1)[18] as a fluorescent guest to be embedded in **2⊂1**, because cyanine dyes are one of the most advantageous NIR fluorochromes frequently employed in cellular imaging and fluorescence sensing.[19] Here, the introduction of adamantyl unit in dye **3** is expected to further enhance the hydrophobicity of the water-repelling segment.

Compounds **1**–**3**, as expected, were simply mixed in aqueous solution to coassemble to ternary supramolecular assembly **3·2⊂1**. The TEM image of **3·2⊂1** showed a number of spherical nanoparticles with an average diameter of 118 nm (Figure S10c, Supporting Information), which is slightly larger than that of **2⊂1** assembly (100 nm). The hydrodynamic diameter of **3·2⊂1** assembly, determined by DLS, was 223 nm (Figure S10d, Supporting Information), which is also larger than that of **2⊂1** assembly (158 nm). These results revealed that **3** was embedded into **2⊂1** assembly to form a larger-sized spherical nanoparticles. It is also to note that the incorporation of **3** into **2⊂1** assembly will not disturb the binding pattern between **1** and **2**, because the bidentate binding of **2** with two PMCDs in **1** is much stronger ($K_S = 7.5 \times 10^5$ M^{-1}) than the monodentate binding of the AD unit in **3** with a PMCD ($K_S < 10^2$ M^{-1}).[20]

Further evidence in support of the formation of ternary assembly comes from the UV–vis and CD spectral examinations. As shown in Figures S14 of the Supporting Information, the introduction of Cy-AD had no effects on the porphyrin's Soret band signals at 375–450 nm in the UV–vis and CD spectra and no appreciable CD signals were induced in the Cy-absorbing region (550–700 nm), revealing that the core of porphyrin **2** is still included by the PMCD cavity of **1**. The possible formation pattern for the nearly spherical nanoparticles of **3·2⊂OF-1** assembly is shown in Scheme 1b.

To our delight, the incorporation of **3** with **2⊂1** assembly to form ternary assembly **3·2⊂OF-1** achieved the dramatic enhancement of NIR fluorescence through FRET. As shown in Figure 2d, when excited at 417 nm to avoid any absorption by Cy-AD (Figure S15a, Supporting Information), the porphyrin fluorescence of **2⊂1** assembly at 647 nm gradually faded out upon addition of **3** and a new emission from cyanine dye **3** emerged at 678 nm (Figure S15b, Supporting Information), indicating occurrence of the FRET process from **2⊂OF-1** assembly to **3**. Visually, the red fluorescence turned to stronger brilliant magenta. The fluorescence intensity at 678 nm reached a plateau upon addition of 3 equivalents of **3** (Figure 2d, inset), revealing the apparent loading capacity of **2⊂1** assembly toward **3** to form ternary assembly [$\mathbf{3}_3\cdot\mathbf{2}\cdot\mathbf{1}$]. The efficiency of energy transfer from **2⊂OF-1**–**3** was determined to be > 84% from the emission intensity decline at 647 nm (Table S3, Supporting Information). In the control experiment, no fluorescence was observed when **3** was excited at 417 nm under a comparable condition (Figure S15c, Supporting Information). Moreover, it is very significant that the quantum yield of **3·2⊂OF-1** ($\Phi_F = 0.21$) is apparently higher than that of **2⊂OF-1** ($\Phi_F = 0.063$), because

high fluorescence quantum yield is always extremely required for biosensing, fluorescent probe, and other light-emitting devices (Table S2, Supporting Information).

The UV–vis spectrum of Cy-AD and the fluorescence spectrum of **2**⊂OF-**1** exhibited a significant spectral overlap in the region 600–700 nm with a perfect match of the emission/excitation 0-0 band at 650 nm (Figure S11b, Supporting Information). To further clarify which noncovalent interaction(s) most significantly contribute to the incorporation of **3** in **2**⊂OF-**1** and therefore to the FRET process between **2**⊂OF-**1** and Cy-AD, we selected host **4**, lacking the positive charge in the triazole segment and tetrakis(*p*-sulfonatophenyl)porphyrin **5**, carrying no alkyl chains, as reference compounds for the control experiments (Scheme S2, Supporting Information). As can be seen from Figure S16 in the Supporting Information, the FRET efficiency as evaluated by the relative intensity of the Cy-AD fluorescence (678 nm) at 8 equivalents, indicating the best effect of **2**⊂OF-**1**. This result reveals that both the electrostatic and hydrophobic interactions are certainly essential in achieving the robust coassembling of the donor (**2**⊂OF-**1**) and the acceptor (**3**).

Interestingly, upon irradiation at 254 nm for 28 s, the strong FRET fluorescence of **3**·**2**⊂**1** was dramatically quenched down to 4% of the original intensity (Figure 2e). Accordingly, the fluorescence color of the solution changed from magenta to dark and the Φ_F of resultant **3**·**2**⊂**1** was greatly reduced from 0.21 to <0.001 (Table S2, Supporting Information). The lifetime was also significantly shortened from 5.3 to 1.2 ns (Figure S9c and Table S2, Supporting Information). These observations jointly suggest that the photocyclization from the open- to the closed-form took place in **3**·**2**⊂**1**. Crucially, the fluorescence intensity, color, lifetime, and quantum yield of the **3**·**2**⊂**1** solution were totally recovered to the original states upon irradiation at >450 nm for 8 min (Figure 2e; Figures S17 and S9c, and Table S2, Supporting Information) attributed to the regeneration of **3**·**2**⊂OF-**1** from **2**·**3**⊂CF-**1**, as was the case with assembly **2**⊂**1**. Moreover, this forward/backward process was repeatable for at least ten times (Figure 2f).

For the photocontrolled FRET process in ternary assembly **3**·**2**⊂**1** are considered two plausible mechanisms, which differ in the quenching of the FRET to dye **3** in **3**·**2**⊂CF-**1** formed upon UV irradiation of **3**·**2**⊂OF-**1** (Scheme 2, right; Figure S18, Supporting Information). In the open-form assembly **3**·**2**⊂OF-**1**, FRET occurs from **2** to **3** to show the magenta fluorescence in the both mechanisms, since OF-**1**, possessing higher excitation energy, never functions as an acceptor. However, once OF-**1** is photocyclized by UV irradiation at 254 nm, the CF-**1** formed becomes a competitor of dye **3** for the FRET from porphyrin **2**. In mechanism [i] (Scheme 2, right), the excitation energy of **2** is directly transferred to nonfluorescent CF-**1**, while two successive FRET processes from **2** to **3** and then to CF-**1** are involved in mechanism [ii] (Figure S18, Supporting Information). Since the fluorescence of **3** and **1** possesses a sensible spectral overlap with the UV–vis spectrum of CF-**1** but not with that of OF-**1** (Figure S11c, Supporting Information), the second mechanism [ii] cannot immediately be ruled out. However, the fluorescence of **3** in **3**·**2**⊂OF-**1** upon excitation at 600 nm did not appreciably change upon UV irradiation at 254 nm for 28 s (where **3**·**2**⊂CF-**1** became the dominant species) (Figure S19, Supporting Information), unambiguously indicating that the energy transfer from **3** to CF-**1** does not occur in ternary assembly **3**·**2**⊂**1** probably due to the interchromophore distance larger than the Förster radius (R_0). Besides, the Förster's theory calculation ($R_{0[2\cdot3]} > R_{0[2\cdot1]}$) further supported the mechanism [i] (Supporting Information). Thus, we conclude that the FRET acceptor is switched by UV irradiation from dye **3** to CF-**1** in **3**·**2**⊂**1**, which is a new approach and different from the other design principles of fluorescent photoswitches in previous reports.[21,15]

In summary, a novel light-responsive ternary nanoparticulate assembly has been elaborately fabricated, where the occurrence of FRET from **2**⊂PMCD (in assembly **2**⊂OF-**1**) to **3** leads to the remarkable enhancement of NIR fluorescence. Significantly, the energy transfer process can be further modulated by photoswitch **1** upon irradiation with distinct light, achieving a photoswitchable NIR fluorescence nanosystem. The present concept and results provide a novel supramolecular strategy for the design and development of photoswitchable photoluminescence materials and are further expandable to the construction of light-triggered logical switches, reciprocating molecular machines, and other photocontrollable molecular devices, by flexibly exchanging the components of the supramolecular system.

Supporting Information

Supporting Information is available from the Wiley Online Library or from the author.

Acknowledgements

The authors thank NNSFC (Nos. 21432004, 21472100, and 91527301) for financial support.

Conflict of Interest

The authors declare no conflict of interest.

Keywords

energy transfer, near-infrared fluorescence, photoswitches, supramolecular assembly

Received: July 20, 2017
Revised: September 15, 2017
Published online:

[1] a) Y. Zeng, Y. Li, M. Li, G. Yang, Y. Li, *J. Am. Chem. Soc.* **2009**, *131*, 9100; b) S. K. Yang, X. Shi, S. Park, T. Ha, S. C. Zimmerman, *Nat. Chem.* **2013**, *5*, 692; c) M. Heilemann, P. Tinnefeld, G. S. Mosteiro, M. G. Parajo, N. F. Van Hulst, M. Sauer, *J. Am. Chem. Soc.* **2004**, *126*, 6514; d) P. M. Holland, R. D. Abramson, R. Watson, D. H. Gelfand, *Proc. Natl. Acad. Sci. USA* **1991**, *88*, 7276; e) B. Dubertret, M. Calame, A. J. Libchaber, *Nat. Biotechnol.* **2001**, *19*, 365.

[2] J. Park, Q. Jiang, D. Feng, L. Mao, H.-C. Zhou, *J. Am. Chem. Soc.* **2016**, *138*, 3518.
[3] a) L. Hou, X. Zhang, T. C. Pijper, W. R. Browne, B. L. Feringa, *J. Am. Chem. Soc.* **2014**, *136*, 910; b) J. Park, D. Feng, S. Yuan, H.-C. Zhou, *Angew. Chem., Int. Ed.* **2015**, *54*, 430.
[4] C. Fan, W. Wu, J. J. Chruma, J. Zhao, C. Yang, *J. Am. Chem. Soc.* **2016**, *138*, 15405.
[5] a) Y. Jiang, J. McNeill, *Chem. Rev.* **2017**, *117*, 838; b) Z. Xu, S. Peng, Y.-Y. Wang, J.-K. Zhang, A. I. Lazar, D.-S. Guo, *Adv. Mater.* **2016**, *28*, 7666; c) H.-Q. Peng, Y.-Z. Chen, Y. Zhao, Q.-Z. Yang, L.-Z. Wu, C.-H. Tung, L.-P. Zhang, Q.-X. Tong, *Angew. Chem., Int. Ed.* **2012**, *51*, 2088; d) Q.-W. Zhang, D. Li, X. Li, P. B. White, J. Mecinović, X. Ma, H. Ågren, R. J. M. Nolte, H. Tian, *J. Am. Chem. Soc.* **2016**, *138*, 13541; e) X. Yao, T. Li, J. Wang, X. Ma, H. Tian, *Adv. Opt. Mater.* **2016**, *4*, 1322.
[6] a) G. Han, D. Kim, Y. Park, J. Bouffard, Y. Kim, *Angew. Chem., Int. Ed.* **2015**, *54*, 3912; b) D. Oushiki, H. Kojima, T. Terai, M. Arita, K. Hanaoka, Y. Urano, T. Nagano, *J. Am. Chem. Soc.* **2010**, *132*, 2795.
[7] M. Chen, M. Zhong, J. A. Johnson, *Chem. Rev.* **2016**, *116*, 10167.
[8] a) M. Irie, T. Fukaminato, K. Matsuda, S. Kobatake, *Chem. Rev.* **2014**, *114*, 12174; b) D.-H. Qu, Q.-C. Wang, Q.-W. Zhang, X. Ma, H. Tian, *Chem. Rev.* **2015**, *115*, 7543; c) B. L. Feringa, R. A. van Delden, N. Koumura, E. M. Geertsema, *Chem. Rev.* **2000**, *100*, 1789.
[9] a) Y. Liu, C.-F. Ke, H.-Y. Zhang, J. Cui, F. Ding, *J. Am. Chem. Soc.* **2008**, *130*, 600; b) H.-L. Sun, Y. Chen, J. Zhao, Y. Liu, *Angew. Chem., Int. Ed.* **2015**, *54*, 9376.
[10] W. Sun, S. Guo, C. Hu, J. Fan, X. Peng, *Chem. Rev.* **2016**, *116*, 7768.
[11] a) K. Kano, H. Kitagishi, S. Tamura, A. Yamada, *J. Am. Chem. Soc.* **2004**, *126*, 15202; b) H. Kitagishi, M. Tamaki, T. Ueda, S. Hirota, T. Ohta, Y. Naruta, K. Kano, *J. Am. Chem. Soc.* **2010**, *132*, 16730.
[12] Y.-X. Wang, Y.-M. Zhang, Y. Liu, *J. Am. Chem. Soc.* **2015**, *137*, 4543.
[13] S. Tomas, L. Milanesi, *J. Am. Chem. Soc.* **2009**, *131*, 6618.
[14] P. Huang, D. Wang, Y. Su, W. Huang, Y. Zhou, D. Cui, X. Zhu, D. Yan, *J. Am. Chem. Soc.* **2014**, *136*, 11748.
[15] L. Giordano, T. M. Jovin, M. Irie, E. A. Jares-Erijman, *J. Am. Chem. Soc.* **2002**, *124*, 7481.
[16] J. Fan, M. Hu, P. Zhan, X. Peng, *Chem. Soc. Rev.* **2013**, *42*, 29.
[17] Z.-Q. Li, Y.-M. Zhang, Y. Chen, Y. Liu, *Chem. Eur. J.* **2014**, *20*, 8566.
[18] M. Sun, H.-Y. Zhang, Q. Zhao, X.-Y. Hu, L.-H. Wang, B.-W. Liu, Y. Liu, *J. Mater. Chem. B* **2015**, *3*, 8170.
[19] M. Bates, B. Huang, G. T. Dempsey, X. Zhuang, *Science* **2007**, *317*, 1749.
[20] M. V. Rekharsky, Y. Inoue, *Chem. Rev.* **1998**, *98*, 1875.
[21] a) H.-B. Cheng, H.-Y. Zhang, Y. Liu, *J. Am. Chem. Soc.* **2013**, *135*, 10190; b) G. Xu, Q.-D. Yang, F.-Y. Wang, W.-F. Zhang, Y.-B. Tang, *Adv. Mater.* **2011**, *23*, 5059; c) T. B. Norsten, N. R. Branda, *J. Am. Chem. Soc.* **2001**, *123*, 1784; d) T. Fukaminato, T. Sasaki, T. Kawai, N. Tamai, M. Irie, *J. Am. Chem. Soc.* **2004**, *126*, 14843; e) D. E. Williams, J. A. Rietman, J. M. Maier, R. Tan, A. B. Greytak, M. D. Smith, J. A. Krause, N. B. Shustova, *J. Am. Chem. Soc.* **2014**, *136*, 11886.

